RESEARCH ARTICLE

Discrimination of metal contaminant sources in river sediments influenced by mining and smelting activities using stable Pb and Zn isotopes

Dong-Jin Joe[1] · Man-Sik Choi[1] · Jong-Hyeon Lee[2] · Chan-Kook Kim[3] · Min-Seok Choi[4] · Hyung-Seon Shin[5]

Abstract

To determine the sources and pathways of lead (Pb) and zinc (Zn) in river sediments contaminated with metals from mining and smelting activities, metal concentrations and Pb and Zn isotope ratios were measured in river water and sediment, and potential metal contaminant samples (imported Zn concentrates, smelting wastes, soils around the smelter, mine ores, and riverside tailings). Zn and cadmium (Cd) concentrations in river water and sediment samples were 30- and 11–25-fold higher, respectively, near the smelter than upstream, while a 6-fold increase in sediment Pb concentrations was detected over the same region. Sediment samples near the smelter ($^{207}Pb/^{206}Pb = 0.8638$ and $^{208}Pb/^{206}Pb = 2.0960$) were observed to have a different Pb isotopic composition from upstream of the smelter ($^{207}Pb/^{206}Pb = 0.8322$ and $^{208}Pb/^{206}Pb = 2.0502$), with $\delta^{66}Zn$ values increasing from –0.01 to 0.82‰. Analysis of Pb and Zn isotopes and concentrations revealed that dust-contaminated soils were a major Pb source, and baseline sediments were found to be contaminated by regional mining tailings. For Zn in sediments, the main Zn sources were groundwater-derived Zn ($\delta^{66}Zn = 1.02 \pm 0.43‰$, n = 4), dust-contaminated soils ($\delta^{66}Zn = –0.18 \pm 0.08‰$, n = 3), and tailings-contaminated sediments ($\delta^{66}Zn = 0.01 \pm 0.07‰$, n = 10). Endmember mixing model results showed that dust-contaminated soils contributed 78% and 64% of sediment Pb and Zn, respectively, within 2 km of the Zn smelter, decreasing to negligible levels after 47.1 km downstream. Downstream of the smelter, groundwater-derived Zn contributed 54% of sediment Zn, whereas tailings contaminated sediments contributed 70% and 25% of Pb and Zn, respectively.

Keywords Forensic · Metal contamination · Metal isotopes · Mine tailings · Sediment · Zinc smelter

Responsible Editor: Luke Mosley

✉ Man-Sik Choi
  mschoi@cnu.ac.kr

1 Department of Marine Environmental Science, Chungnam National University, Daejeon 34134, Republic of Korea

2 Environmental Human Research & Consulting (EHR&C), Incheon 22689, Republic of Korea

3 Marine Environment Research Institute, OCEANIC C&T Co., Ltd, Seoul 07207, Republic of Korea

4 Marine Environment Monitoring Team, Korea Marine Environment Management Corporation, Busan 49111, Republic of Korea

5 Center for Research Equipment, Korea Basic Science Institute, Cheongju-Si, Chungbuk 28119, Republic of Korea

Introduction

Metal sources in the environment can be traced using a variety of methods, including estimating spatiotemporal gradients of metal concentrations and relative enrichment factors, metal association and receptor models such as principal component analysis, and quantitative contribution analysis based on stable isotopic composition, which is a direct indicator of contaminant sources (Chen et al. 2022; Liu et al. 2020; Zhang et al. 2016; Zhong et al. 2021). Although these methods are complementary, a multiple isotope approach can provide integrated information about contaminant sources and transport pathways (Chen et al. 2022; Shiel et al. 2010; Šillerová et al. 2017; Souto-Oliveira et al. 2018; Wang et al. 2021). For example, Pb has four stable isotopes including non-radiogenic ^{204}Pb and three radiogenic isotopes (^{206}Pb, ^{207}Pb, and ^{208}Pb) that are formed through the radioactive decay of uranium and thorium isotopes (Dickin 1995). Therefore, various Pb sources may have unique isotopic

compositions that allow the determination of natural or anthropogenic Pb emission source contributions in environmental medias such as sediments (Choi et al. 2007a, b; Townsend and Seen 2012), soils (Klaminder et al. 2011; Morton-Bermea et al. 2011), plants (Bindler et al. 2004; Weiss et al. 1999), and aerosols (Monna et al. 1997). Zn has five isotopes (^{64}Zn, ^{66}Zn, ^{67}Zn, ^{68}Zn, and ^{70}Zn) that are subjected to isotopic fractionation during ore genesis (Sonke et al. 2008; Wilkinson et al. 2005), biogeochemical processes (Arnold et al. 2010; Jouvin et al. 2012; Juillot et al. 2008), and anthropogenic processes such as smelting (Shiel et al. 2010; Weiss et al. 2007), combustion (Mattielli et al. 2009; Ochoa Gonzalez and Weiss 2015), and electroplating (Araújo et al. 2017; Kavner et al. 2008; Tonhá et al. 2020), leading to isotopic fingerprints that allow differentiation from natural isotopic compositions (Yin et al. 2016). High-temperature processes such as ore roasting and smelting tend to fractionate Zn isotopes, with lighter isotopes predominating atmospheric emissions and heavier isotopes accumulating in slags and effluents (Borrok et al. 2010; Ochoa Gonzalez and Weiss 2015; Sonke et al. 2008; Yin et al. 2016). In contrast, high-temperature geological processes such as magmatic differentiation do not significantly fractionate Zn isotopes, resulting in homogeneous Zn isotopic composition in the bulk Earth (Chen et al. 2013). Zn released into the environment is also isotopically fractionated through biogeochemical processes such as adsorption, dissolution, and biological uptake (Arnold et al. 2010; John et al. 2007; Jouvin et al. 2012; Juillot et al. 2008). Thus, Zn isotopes can be used to trace the pathways and sources of contaminants derived from various sources such as smelting or mining, and a combination of isotopic information from different metals (e.g., Pb and Zn) can provide complementary information about contaminant sources and pathways that may be used to quantitatively estimate source contributions.

The upper reaches of the Nakdong River on the southeastern Korean peninsula feature many abandoned non-ferrous metal mines and an active Zn smelter. Because these operations have continued for over 60 years, related heavy metal contamination has been reported in soils (Jeon et al. 2017; Kang et al. 2019), river water (Kim et al. 2016), groundwater (Song et al. 2023), fish (Kwon et al. 2022), and river and lake sediments (Choi et al. 2015). This heavy metal contamination has emerged as a social problem, and several studies have been conducted to identify its sources. Zn concentrations and Pb isotopes have been used as indicators of smelter-generated materials in soils (Jeon et al. 2017; Kang et al. 2019). However, metal source contaminants in sediments have remained controversial. For example, chemical compositions in sediments and river water (Kim et al. 2016) and Pb isotope levels in lake sediments (Park et al. 2012) demonstrated that sediment metal composition was affected by mine tailings, whereas a contamination history of Zn,

cadmium (Cd), and Pb in lake sediments showed a shift from mining- to smelting-derived metals as the dominant contaminants over time (Choi et al. 2015). Therefore, new indicators should be developed to discriminate metal contaminant sources and estimate the contribution of smelting-derived materials to river and lake sediments to improve the performance of environmental forensic investigations. In this study, we discriminated smelting and mining activities as sources of Pb and Zn contaminants in a segment of the Nakdong River, determined their pathways to the environment, and estimated the contribution of each source to river sediments according to Pb and Zn isotopic compositions.

Materials and methods

Study area

The study area (36° 43′ 29.3″–37° 5′ 42.3″ N, 128° 50′ 49.2″–129° 5′ 48.3″ E) was an upper segment of the Nakdong River on the southeastern Korean peninsula, approximately 100 km upstream from the entrance to Lake Andong, which is an artificial reservoir created by the construction of the Andong Dam in 1976 (Fig. 1). Approximately 100 mines were in operation within this drainage area during the 1970s and 1980s, but have been abandoned continuously since 1988. To date, 95 mines (55% metal, 39% non-metal, and 6% coal) have been abandoned (Kim et al. 2022). Among these, the Yeonhwa (508,000 tons Pb and 975,000 tons Zn) and Janggun mines (141,000 tons Pb and 264,000 tons Zn) produced the largest volume of Pb–Zn bulk concentrates in Korea, as well as approximately 2,000,000 m^3 of tailings and 4,000,000 m^3 of rock wastes, which accumulated near the mines and their adjacent rivers (Kim et al. 2022). In 1972, typhoon-related flooding led to a large-scale discharge of contaminants into the Nakdong River, followed by the deposition of 8,840 m^3 of mine tailings along the 91 km river floodplain from a Zn smelter to the entrance of Lake Andong (Hong et al. 2016; Kim et al. 2016). Korea's largest Zn smelter, established in 1970, is still operational, with an annual production capacity of 350,000 tons of Zn ingots through continuous facility expansion. The Zn smelter facilities include ore storage for Zn concentrates imported by truck and rail, as well as a wide exposed area where smelting waste is stored for later generation of by-products. The smelter once produced pure Zn from Zn concentrates derived from local mines; however, > 98% of the total Zn production now depends on imported Zn concentrates.

Materials

River waters (18 main channels and 13 tributaries, W1-W31) and sediments (45 main channels and 13 tributaries, N1-N58) were collected from 10.2 km upstream to 90.3 km

Fig. 1 Map of river water and sediment sampling sites in the study area. A total of 31 water samples (18 main channels and 13 tributaries) and 58 sediment samples (45 main channels and 13 tributaries) were collected in August and May 2020. Smelter and abandoned metal mines are indicated by red rectangle box and open stars, respectively. The outlet of treated wastewater in the smelter, located about 0.50 km downstream from the Zn smelter plant 1 (N12 and W8), is represented by a red star
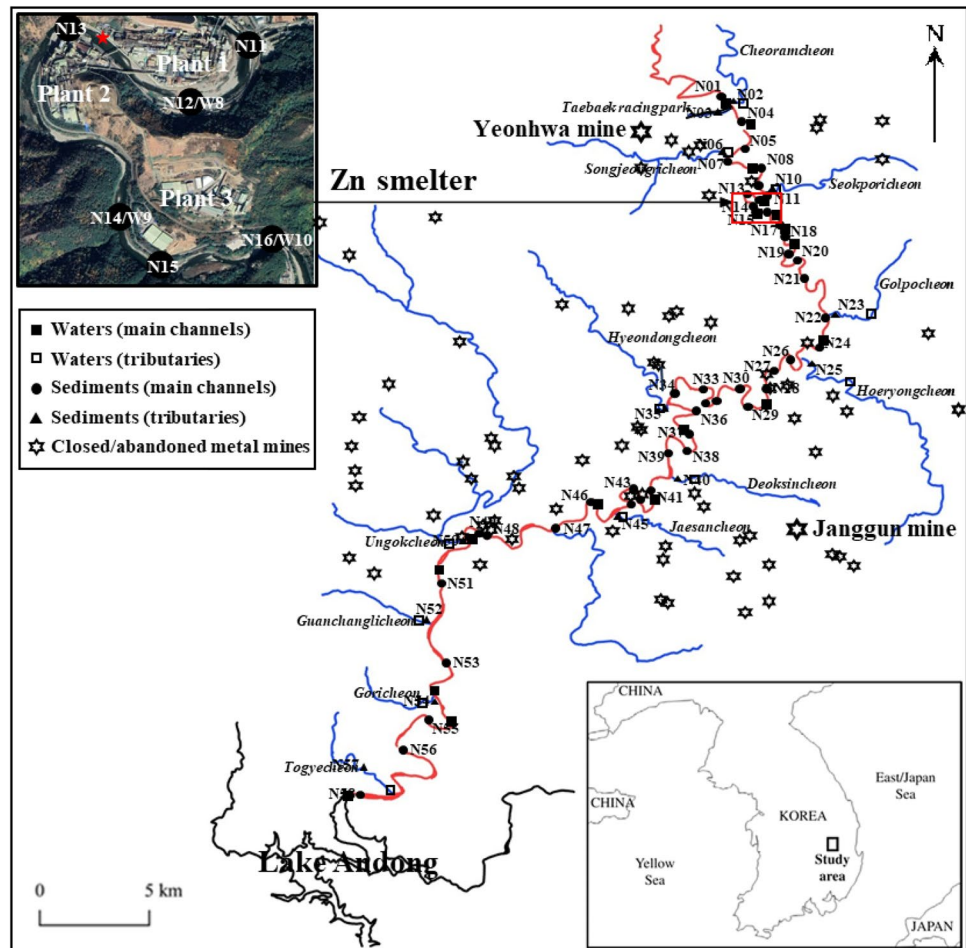
downstream of the Zn smelter in May and August 2020 (Fig. 1). River waters were collected using a pole sampler or horizontal Van Dorn sampler and then filtered on site into 125 mL acid-washed low-density polyethylene bottles using acid-washed syringe filters (pore size 0.45 μm) and syringes, and the filtrates were acidified with purified HNO_3 and transported to the laboratory. To evaluate the possibility of metal-contaminated groundwater from the smelter directly into the river, river waters (n = 5) were also collected from a cross-section of the Nakdong River at station W8 (i.e., at the Zn smelter). Sediments were collected using a plastic scoop and grab sampler, and samples for grain size fraction and total organic carbon (TOC) analysis were wet-sieved through a 2 mm sieve, while samples for chemical analysis were sieved to 150 μm fractions, which is the standard operating procedure for reporting and measuring total heavy metal concentration in soil under the Korean Ministry of Environment. Samples of imported Zn concentrate (n = 7), smelting waste (n = 4), and soil around the Zn smelter (0–2 cm depth, n = 3), which are possible metal contaminants, were collected from the concentrate storage and smelting waste storage located inside plant 1 and from a hillside approximately 0.50 km

from the smelter, respectively. For the Korean mine ores (n = 9) and riverside tailings (n = 7), samples were collected from six abandoned metal mines and from tailings deposited at the riverside of a main channel. All sediment and possible metal contaminant samples were transported to the laboratory, freeze-dried and powdered, and stored until chemical analysis.

Methods

Grain size fraction was calculated as the percentage of each fraction to dry weight by treating sediment samples (< 2 mm) with a 30% H_2O_2 solution and sieving through 150- and 63-μm sieves. TOC was determined using an automated elemental analyzer (Flash 2000 Series, Thermo Scientific, Waltham, MA, USA) after carbonates were removed using high purity water and H_2SO_3 (Nieuwenhuize et al. 1994; Verardo et al. 1990). Powdered sediment samples (< 150 μm) were determined for lithium (Li), Pb, Zn, and Cd concentrations through inductively coupled plasma mass spectrometry (ICP–MS, ELAN DRC II, PerkinElmer Inc.) after total digestion with mixed acids (HF:HNO_3:$HClO_4$,

4:4:1). Filtered and acidified river water samples were directly analyzed for Pb, Zn, and Cd using ICP–MS (ELAN DRC II). Certified reference materials including NRCC SLRS-6 and NIST SRM 1640a for water and USGS BCR-2, NRCC PACS-2, and NIST SRM 2711a for sediment were analyzed with samples together, with metal recoveries ranging from 85 to 110% (Supplementary Table 1 and 2).

Powdered sediment samples (200 mg) for Pb and Zn isotope analysis were weighed in low-pressure teflon digestion vessels (Savillex, Eden Prairie, MN, USA) and digested with 5 mL HF and 5 mL aqua regia at 180 °C for 24 h. After digestion, the strong acids were dried and residues were extracted with 1 M HCl, and then centrifuged at 3,000 rpm for 10 min, and the supernatants were collected. For Pb isotope analysis, the solutions were diluted with 0.5 M HNO_3 to achieve a total dilution factor of 2,000. Solutions for Zn isotope analysis were transferred to perfluoroalkoxy alkane vials and evaporated at 120 °C on a hot plate; the residues were redissolved in 1 mL of 2 M HCl for Zn separation. For the Zn column, we used a poly prep column (Bio-Rad, Hercules, CA, USA) packed with 2 mL AGMP-1 resin (Bio-Rad; 100–200 mesh, chloride form). To improve the accuracy and precision of Zn isotope analysis, we minimized potential interference using a second column (Supplementary Table 3). The separated Zn fractions were then evaporated at 120 °C and dissolved in 0.5 M HNO_3. Pb and Zn isotopes were analyzed using a multicollector ICP–MS (Neptune Plus, Thermo Scientific) at Korea Marine Environment Management Corp. (Busan, South Korea). To correct mass bias, external normalization method was applied to standards and samples (Chen et al. 2016; Maréchal et al. 1999; Mason et al. 2004). Prior to analysis, all samples were doped with thalium (NIST SRM 997) at a concentration of 10 ng/mL for Pb, and with Cu (ERM-AE 647) at a 1:1 Zn:Cu ratio and concentration of 50 ng/mL for Zn. To minimize concentration effects, the Zn concentrations of standards and samples were matched to within ± 5%.

Zn isotopic compositions are commonly reported using δ notation, which expresses deviation (‰) from the isotopic standard (IRMM 3702) as follows:

$$\delta^{66}Zn_{IRMM3702}(‰) = \left(\frac{\left(\frac{^{66}Zn}{^{64}Zn} \right)_{sample}}{\left(\frac{^{66}Zn}{^{64}Zn} \right)_{IRMM3702}} - 1 \right) \times 1000 \quad (1)$$

The external reproducibility of these methods was evaluated using NIST SRM 981 for Pb isotopes, and NIST SRM 682, USGS BCR-2 (basalt), NRCC PACS-2 (sediment), and NIST SRM 2711a (soil) for Zn isotopes. The NIST SRM 981 solution was measured once every five samples to ensure that the instrument's measurement accuracy was maintained; we obtained Pb isotopic values of $^{207}Pb/^{206}Pb = 0.9147 \pm 0.0001$

and $^{208}Pb/^{206}Pb = 2.1668 \pm 0.0004$ (n = 75), which align with those reported previously ($^{207}Pb/^{206}Pb = 0.9146 \pm 0.0001$ and $^{208}Pb/^{206}Pb = 2.1671 \pm 0.0004$; Todt et al. 1996). The repeatability of the Zn isotope analysis was verified by measurements on IRMM 3702 ($\delta^{66}Zn_{IRMM3702} = 0.00 \pm 0.02‰$, n = 102) and NIST SRM 682 ($\delta^{66}Zn_{IRMM3702} = -2.66 \pm 0.12‰$, n = 11); the results were within the analytical error of the certified values (John et al. 2007; Tanimizu et al. 2002). The $\delta^{66}Zn$ values of three geological reference materials relative to IRMM 3702 are provided in Supplementary Table 4.

Results

Geochemical properties of river sediments

Grain size fractions and TOC contents in bulk sediments (< 2 mm), and Li concentrations in < 150 μm sediments sampled from 45 main channel sites and 13 tributary sites are presented in Supplementary Fig. 1. In the main channel, the average 2 mm to 150 μm, 150 to 63 μm and < 63 μm grain size fractions were 94.6 ± 7.05%, 5.43 ± 7.05% and 1.34 ± 2.90%, respectively. In tributaries, the average 2 mm to 150 μm grain size fraction was 96.3 ± 2.96%, and that for < 63 μm was 1.34 ± 1.59%. The average TOC content in main channel bulk sediments (< 2 mm) was 0.53 ± 0.47%, with no clear trend; its distribution was independent of the fine-grained (< 63 μm) sediment distribution (r = 0.22). However, the average TOC content in tributaries (0.33 ± 0.31%, n = 13) was significantly correlated with fine-grained sediment fraction (r = 0.83). Li concentrations in sediments (< 150 μm) sampled from the main channel (n = 45) and tributaries (n = 13) ranged from 11.1 to 90.2 mg/kg (average, 50.9 ± 13.8 mg/kg) and 37.2 to 87.0 mg/kg (average, 60.5 ± 14.9 mg/kg), respectively. No clear trend was observed for Li distribution, which was independent of the fine-grained sediment distribution (r = 0.31).

Metal concentrations in river waters and sediments

Dissolved Pb, Zn, and Cd concentrations in river waters collected in the main channel (n = 18) and tributaries (n = 13) are shown in Fig. 2a–c. From -9.73 to -3.11 km upstream of the smelter, dissolved metal concentrations were consistently very low (0.01 ± 0.01 μg/L for Pb, 5.94 ± 0.95 μg/L for Zn, and 0.03 ± 0.01 μg/L for Cd, n = 3). Zn and Cd concentrations increased rapidly from the smelter to downstream reaches, with maximum concentrations at stations W12 (5.18 km downstream of the smelter, Zn concentration, 123 μg/L) and W9 (1.75 km downstream of the smelter, Cd concentration, 3.33 μg/L), and then decreased exponentially further downstream. A slight Pb concentration increase

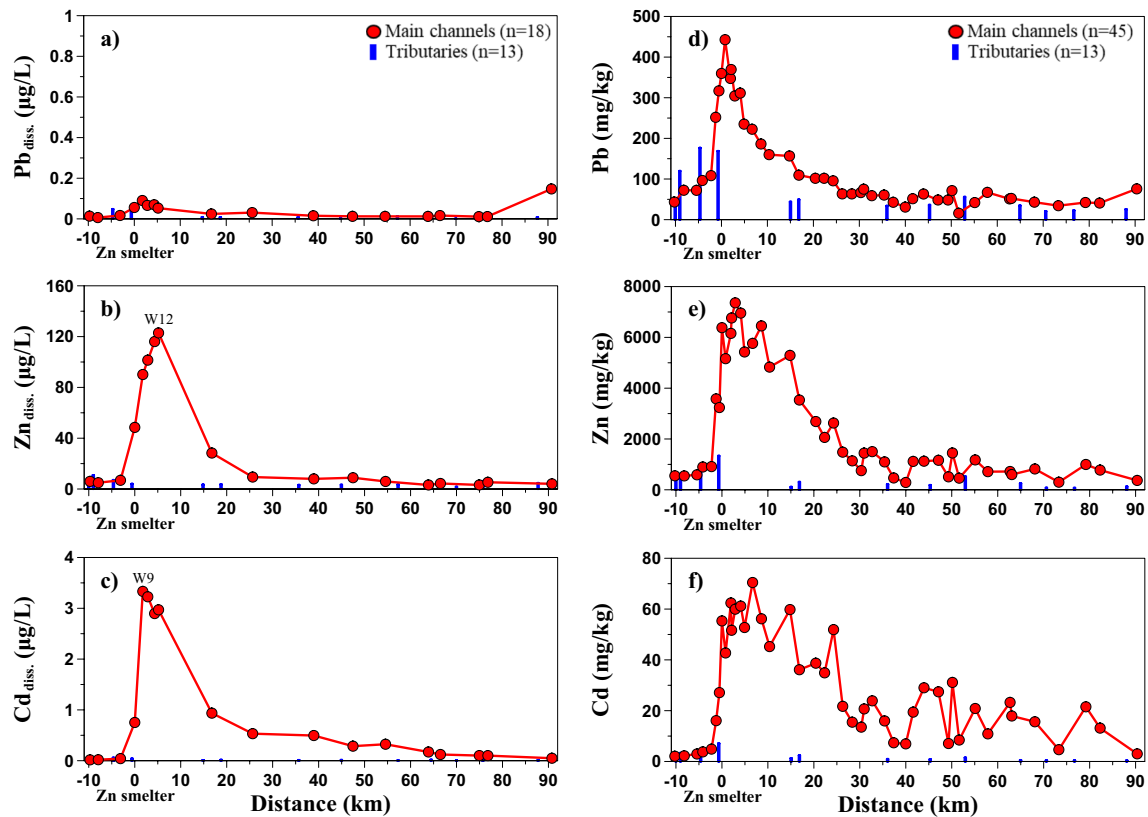**Fig. 2** Pb, Zn and Cd concentrations in river waters (**a**, **b** and **c**) and sediments (<150 μm fraction; **d**, **e** and **f**). Each sampling location is presented along the relative distances from the Zn smelter plant 1 (W8 and N12, respectively), positive and negative for downstream and upstream, respectively

was observed near the Zn smelter; however, Pb concentrations were generally very low (average, 0.04 ± 0.04 μg/L). In tributaries, Pb, Zn, and Cd concentrations were consistently very low, with averages of 0.01 ± 0.01, 4.38 ± 2.36, and 0.01 ± 0.02 μg/L, respectively, which were similar to those in the upper reaches. Dissolved metal concentrations in water sampled near the smelter (station W8, n = 5) were 15-fold higher for Cd and 2-fold higher for Zn on the Zn smelter side of the river cross-section than on the road side, whereas Pb concentrations were consistently very low (Supplementary Fig. 2). These results suggest that groundwater with very high concentrations of Cd and Zn flows directly from the interior of the Zn smelter to the main channel of the Nakdong River, which is consistent with the results of a groundwater leakage investigation that performed bromide and uranine tracer tests and groundwater modeling (Song et al. 2023).

Pb, Zn, and Cd concentrations in river sediments (<150 μm) from the main channel (n = 45) and tributaries (n = 13) are shown in Fig. 2d–f and Supplementary Table 5. Pb, Zn, and Cd concentrations from -10.2 to -2.27 km upstream of the smelter were low and constant, with averages of 78.5 ± 25.0, 699 ± 188, and 3.18 ± 1.16 mg/kg

(n = 5), respectively. From station N9 (-1.26 km upstream of the smelter), the concentrations of all three metals increased rapidly as distance to the Zn smelter decreased, reaching maximum concentrations at station N13 for Pb (443 mg/kg), N16 for Zn (7,360 mg/kg), and N19 for Cd (70.5 mg/kg). Downstream of the smelter, Pb concentrations decreased rapidly, and Zn and Cd maintained high concentrations for a distance of ~15 km and then decreased linearly to ~40 km and maintained low concentrations until the entrance of Lake Andong. Zn and Cd concentrations were much lower in the tributaries than in the main channel, with similar levels to the main channel upstream of the smelter. Pb concentrations were higher in upstream tributaries, but much lower than in the main channel near the smelter. Pb, Zn, and Cd distributions in river sediments (<150 μm) differed greatly from those of the fine-grained fraction (r = –0.14, –0.20, and –0.22, respectively) and TOC content (r = 0.04, 0.13, and 0.07, respectively), such that high metal concentrations may have been caused by their direct supply from the Zn smelter, rather than compositional relationships such as preferential association of metals with fine-grained sediments and organic matter (Horowitz 1991).

^{207}Pb/^{206}Pb, ^{208}Pb/^{206}Pb, and δ^{66}Zn in river sediments

Pb and Zn isotope ratios in main channel sediments (< 150 μm) varied greatly at the Zn smelter (Fig. 3) in a manner similar to their concentrations. From -10.2 to -2.27 km upstream of the smelter, the average Pb isotope ratios were 0.8322 ± 0.0067 (n = 5) for ^{207}Pb/^{206}Pb and 2.0502 ± 0.0190 (n = 5) for ^{208}Pb/^{206}Pb; the average δ^{66}Zn value was 0.01 ± 0.03‰ (n = 4). From -1.26 km upstream (N9) to 14.8 km downstream (N22) of the smelter, Pb concentrations rapidly increased and then decreased (Fig. 2d), and Pb isotope ratios were consistently high, with averages of 0.8638 ± 0.0052 for ^{207}Pb/^{206}Pb and 2.0960 ± 0.0096 for ^{208}Pb/^{206}Pb (n = 13) in main channel sediments. At Seokporicheon (N10), a tributary near the Zn smelter, Pb isotope levels were also above average. At 47.1–90.3 km downstream of the smelter, Pb isotope ratios were low and highly variable, apparently influenced by nearby tributaries. Zn isotope ratios increased rapidly along with Zn concentrations at -1.26 km upstream of the smelter, and the highest δ^{66}Zn value was observed at 8.59 km downstream of the smelter (N20, δ^{66}Zn = 0.82‰). A slight decrease in Zn isotope ratios occurred from 14.8 to 90.3 km downstream of the smelter (δ^{66}Zn = 0.56 ± 0.12‰), although Zn concentrations decreased exponentially. Interestingly, stations N9, N10, and N11 near the smelter had a δ^{66}Zn value of -0.01 ± 0.00‰, despite their high Zn concentrations (average, 2720 ± 1210 mg/kg, n = 3). Tributary samples had highly variable Pb isotope ratios, with averages of 0.8180 ± 0.0430 for ^{207}Pb/^{206}Pb and 2.0353 ± 0.0953 for ^{208}Pb/^{206}Pb (n = 12). The average δ^{66}Zn was 0.00 ± 0.08‰

(n = 7) from -10.2 km upstream to 53.0 km downstream of the smelter, excluding the Seokporicheon tributary (N10) and 53.0–90.3 km downstream of the smelter, with an average of -0.32 ± 0.06‰ (n = 5).

Pb and Zn isotope fingerprints of sources

Pb and Zn isotopic compositions of potential metal contaminant source materials including imported Zn concentrates, Korean mining ores, smelting wastes, and dust-contaminated soils sampled near the Zn smelter are shown in Fig. 4 and Supplementary Table 6. Imported Zn concentrates (Zn concentration > 40%) used in the Zn smelter had a wide range of Pb isotopic compositions (0.7559–0.9629 for ^{207}Pb/^{206}Pb and 1.8992–2.2367 for ^{208}Pb/^{206}Pb, n = 36; Kang et al. 2019), and many Zn concentrates lie on the worldwide growth curve of Pb ores such as galena in Australia, Peru, Mexico and USA (Cumming and Richards 1975). The Pb isotopic compositions of Korean ores (0.7827–0.8625 for ^{207}Pb/^{206}Pb and 1.9319–2.1464 ^{208}Pb/^{206}Pb, n = 98; Jeong et al. 2012; Kang et al. 2019; Park and Chang 2005) and riverside tailings (0.8133–0.8200 for ^{207}Pb/^{206}Pb and 2.0108–2.0233 for ^{208}Pb/^{206}Pb, n = 8; NIER, 2011) are situated along the Korea ore line. The difference between these ore curves was consistent with previous studies that showed higher ^{208}Pb levels in Pb–Zn deposits on the Korean peninsula than indicated by a Pb growth curve (Choi et al. 2007a, b; Mukai et al. 1993). Pb isotopic compositions of smelting wastes (0.8712–0.9053 for ^{207}Pb/^{206}Pb and 2.1120–2.1565 for ^{208}Pb/^{206}Pb, n = 17; MOE, 2016) and residential roof dusts and dust-contaminated soils (0.8590–0.9014 for ^{207}Pb/^{206}Pb and 2.1030–2.1525 for ^{208}Pb/^{206}Pb, n = 20;
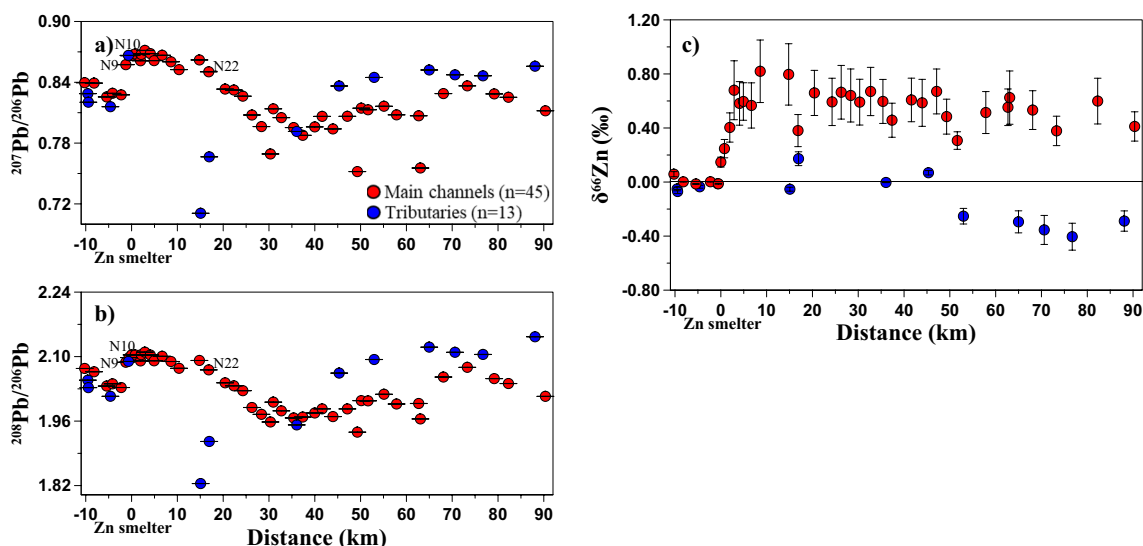

Fig. 3 Pb (**a** and **b**) and Zn (**c**) isotope ratios of the river sediments (< 150 μm fraction). Each sampling location is presented along the relative distances from the Zn smelter plant 1 (N12), positive and negative for downstream and upstream, respectively

Fig. 4 $^{207}Pb/^{206}Pb$ vs. $^{208}Pb/^{206}Pb$ ratios of the river sediments. Pb contaminants including global lead ores (Kang et al. 2019), imported Zn concentrates (Kang et al. 2019; this study), Korean ores (Ores from Yeonhwa, Janggun and other mines; Park and Chang 2005; Jeong et al. 2012; Kang et al. 2019; this study), smelting wastes (MOE, 2016; this study), residential roof dusts (Kang et al. 2019), dust-contaminated soils (this study) and riverside tailings (NIER 2011; this study) are indicated
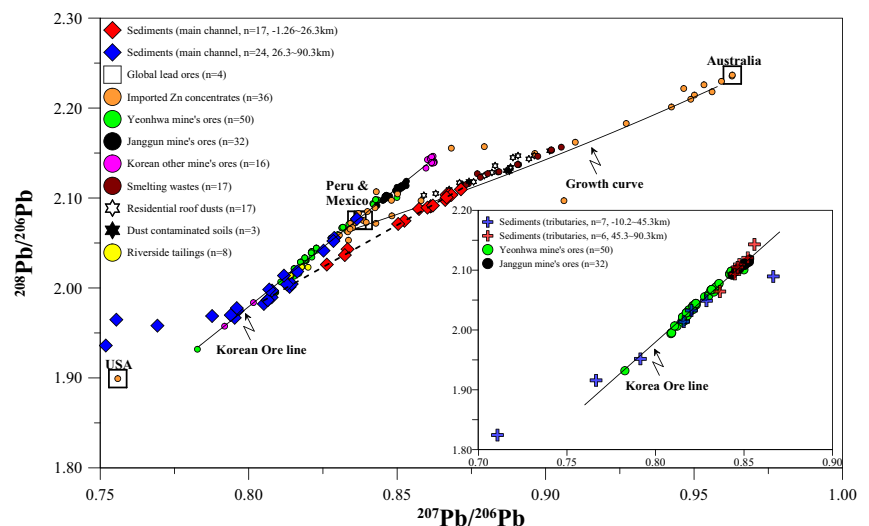
Kang et al. 2019; MOE, 2016) were similar to the mean values (0.8756 ± 0.0538 for $^{207}Pb/^{206}Pb$ and 2.1211 ± 0.0739 for $^{208}Pb/^{206}Pb$) of imported Zn concentrates (n = 36) used in the Zn smelter.

The Zn isotopic compositions of imported Zn concentrates were divided into two groups, with $\delta^{66}Zn$ of $-0.18 \pm 0.04‰$ (n = 5) and $-0.51 \pm 0.02‰$ (n = 2), respectively (Supplementary Fig. 3). The former value is similar to the global median for Zn sulfide (ZnS) ores, which have an interquartile range (IQR) of -0.35 to $-0.08‰$ and a median of $-0.17‰$ (n = 97) (Aranda et al. 2012; Deng et al. 2017; Duan et al. 2016; Gagnevin et al. 2012; John et al. 2008; Kelley et al. 2009; Maréchal et al. 1999; Mason et al. 2005; Mondillo et al. 2018; Pašava et al. 2014; Sivry et al. 2008; Skierszkan et al. 2016; Sonke et al. 2008; Zhu et al. 2018). Although the sample size of the latter group was very small, its value was similar to the mean for Korean mining ores ($\delta^{66}Zn = -0.55 \pm 0.08‰$, n = 9). This difference may be attributed to variation in the formation mechanisms of ZnS ores in different Pb–Zn deposits (Zhang et al. 2022). The Zn isotopic compositions of riverside tailings were also divided into two groups, with $\delta^{66}Zn$ values of $-0.09 \pm 0.10‰$ (n = 5) and $-0.49 \pm 0.04‰$ (n = 2). The former value is similar to that of bulk silicate earth (BSE) ($-0.04 \pm 0.05‰$ of $\delta^{66}Zn$; Chen et al. 2013) and the latter is similar to the average $\delta^{66}Zn$ values of Korean mining ores (Supplementary Fig. 3). Dust-contaminated soils collected near the Zn smelter, had very high Zn concentrations (2900 ± 2260 mg/kg, n = 3) and low $\delta^{66}Zn$ ($-0.18 \pm 0.08‰$, n = 3). Smelting wastes had highly variable $\delta^{66}Zn$ values ($0.73 \pm 0.43‰$, n = 4), indicating wide variation in Zn isotope fractionation during smelting. However, these values were consistent with the range of $\delta^{66}Zn$ values for smelting sludge and effluents reported in the literature, with an IQR of 0.51–1.18‰ and

median of 0.69‰ (n = 16; Desaulty and Petelet-Giraud 2020).

Discussion

Identification of Pb and Zn sources and pathways

To confirm Pb and Zn sources, the relationships between metal isotope ratios and the reciprocal of metal concentrations were shown in Fig. 5. For Pb (Fig. 5a and Supplementary Fig. 4), sediments near the Zn smelter (-1.26 km upstream to 26.3 km downstream, n = 17) showed a strong linear relationship with the Li/Pb ratio ($Y = -0.09X + 0.88$, $r^2 = 0.88$ for $^{207}Pb/^{206}Pb$ and $Y = -0.16X + 2.12$, $r^2 = 0.86$ for $^{208}Pb/^{206}Pb$), indicating the mixing of two sources. The Y-intercept values indicated Pb isotopic compositions consistent with Zn smelter materials, including imported Zn concentrates, smelting wastes, residential roof dusts, and dust-contaminated soils. However, Pb leaching from smelting wastes to groundwater was ruled out as a source of Pb contamination due to negligible transport of dissolved Pb (Fig. 2a), and discharges of imported Zn concentrates and smelting wastes appear unlikely given the management practices at the Zn smelter (MOE 2016). Thus, atmospheric deposition of smelting dust appears to be a main pathway of Pb supply from the smelter to the river, and since soils within a radius of 2 km from this smelter were severely contaminated by dust emitted from the smelter (Kang et al. 2019), runoff of dust-contaminated soils was considered to be the major source of Pb. According to Fig. 5a, the sediment baseline levels were determined to be 57.6 ± 12.7 mg/kg for Pb concentration, 0.7971 ± 0.0126 for $^{207}Pb/^{206}Pb$, and 1.9775 ± 0.0127 for $^{208}Pb/^{206}Pb$ (n = 10) (Supplementary Fig. 4). Thus, baseline levels were detected in sediments
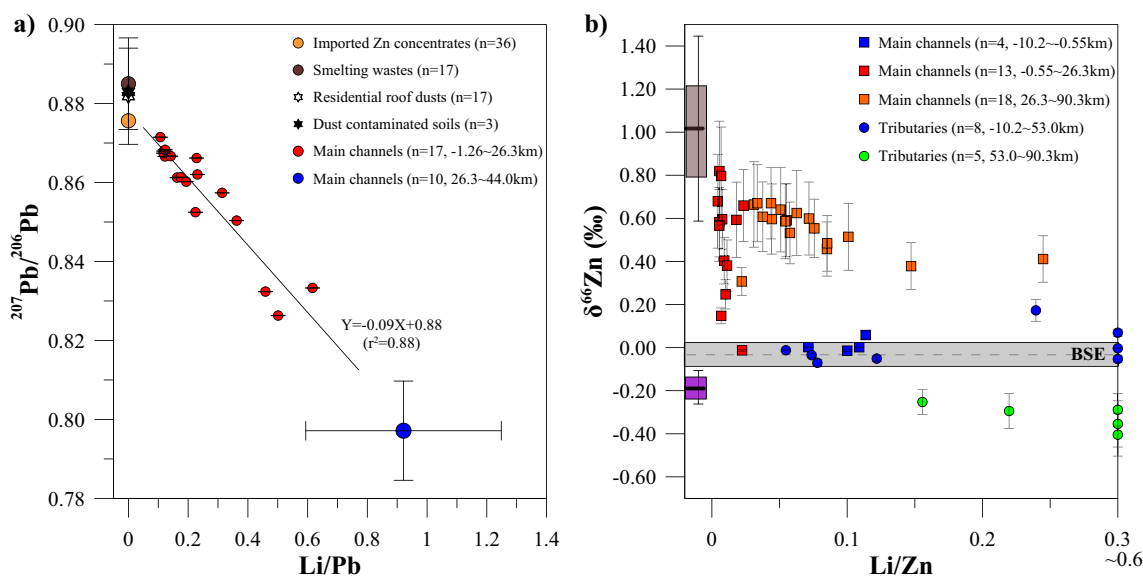
Fig. 5 $^{207}Pb/^{206}Pb$ *vs.* Li/Pb ratios (**a**) and $\delta^{66}Zn$ *vs.* Li/Zn ratios (**b**) of the river sediments. Error bars represent the 2σ associated with $^{207}Pb/^{206}Pb$ ratios and $\delta^{66}Zn$ values. In figure (**a**), Pb contaminants including imported Zn concentrates (Kang et al. 2019; this study), smelting wastes (MOE, 2016; this study), residential roof dusts (Kang et al. 2019) and dust-contaminated soils (this study) are indicated, and baseline sediments were also designated. In figure (**b**), the gray

line labeled "BSE" represents the mean of bulk silicate earth ($\delta^{66}Zn$ $-0.04 \pm 0.05‰$; Chen et al. 2013). Zn contaminants are shown with a purple box plot for dust-contaminated soils ($\delta^{66}Zn$ $-0.18 \pm 0.08‰$, n=3) and a dark brown box plot for the estimated values ($\delta^{66}Zn$ $1.02 \pm 0.43‰$, n=4) of Zn adsorbed from groundwater originating from smelting wastes (FeOOH: $\Delta^{66}Zn_{solid-solution} \sim 0.29‰$; Juillot et al. 2008)

from 26.3 to 44.0 km downstream of the smelter, indicating little influence of Zn smelter materials. However, Pb concentrations were approximately 2-fold higher in the baseline sediments than in the background soils (20.6 ± 4.70 mg/kg for Pb, 0.7794 ± 0.0431 for $^{207}Pb/^{206}Pb$, and 1.9385 ± 0.1224 for $^{208}Pb/^{206}Pb$; Kang et al. 2019), and their isotope ratios were less radiogenic, so the baseline sediments were defined as contaminated by the riverside tailings, which were frequently observed along the main channel of the river. Metal contamination of river sediments by mine tailings was similar to cases reported at the Sasa mine in North Macedonia, the Mount Polley gold and copper mine in British Columbia-Canada, and an iron mine in southeastern Brazil (Byrne et al. 2018; Duarte et al. 2021; Vrhovnik et al. 2013). Although the Pb isotopic compositions of sediments in tributaries were also plotted along the Korean ore line (Fig. 4), there was a difference in Pb isotopic compositions between tributaries upstream (10.2–45.3 km) and downstream (45.3–90.3 km), which were presumably caused by regional differences in the bedrock and sedimentary rock of the study area (Park and Chang 2005; Supplementary Fig. 5).

For Zn, sediments near the Zn smelter (-0.55 km upstream to 26.3 km downstream, n = 13) had very high Zn concentrations (Li/Zn < 0.02), with a wide range of $\delta^{66}Zn$ values (–0.01 to 0.82‰) (Fig. 5b). The linear trend in these samples indicates mixtures of two or more contaminant sources: dust-contaminated soils,

groundwater contaminated through leaching of stored wastes, and tailings from nearby abandoned mines; these had lighter, heavier, and unfractionated Zn isotopes from BSE (–0.04 ± 0.05‰ of $\delta^{66}Zn$; Chen et al. 2013), respectively. As observed for Pb, dust-contaminated soil (–0.18 ± 0.08‰, n = 3) was a source of contamination, which is similar to a case of metal contamination in river sediments due to contaminated soil wash-out around a smelter in the Baiyin region of China (Zhao et al. 2020). The flow of groundwater contaminated with smelter-derived metals into the main channel of the Nakdong River (MOE 2020a; Song et al. 2023; Supplementary Fig. 2) indicates that Zn derived from groundwater containing metals leached from smelting wastes was adsorbed onto sediments. Baseline sediments (Zn concentration = 476 ± 255 mg/kg, $\delta^{66}Zn$ = 0.01 ± 0.07‰, n = 11, blue square and circle symbols in Fig. 5b, excluding Seokporicheon tributary) containing riverside tailings are also an important contamination source. Thus, Zn contaminants are composed of a mixture of three components: dust-contaminated soils, groundwater-derived Zn, and baseline sediments. Sediments from 26.3 to 90.3 km downstream of the smelter contained a minimal contribution from dust-contaminated soils, as shown by the lack of a Pb signal. Thus, groundwater-derived metals were an important Zn source in this zone. This result was similar to those of other studies showing that fluvial dispersion

of contaminants from Zn smelter was detected over much greater distances than the effects of atmospheric dispersion (Foucher et al. 2009; Žibret and Šajn 2008).

Estimation of source contributions

If the major metal contaminant sources and isotope ratios are identified, the contributions of two or three components can be quantitatively estimated using mixing equations (Zhang et al. 2016). Using this method, the Pb signals from -1.26 km upstream to 26.3 km downstream of the smelter was interpreted as a mixture of Pb from dust-contaminated soils and baseline sediments. Thus, the quantitative contribution of each Pb source in this zone was estimated as follows:

$$f_1 + f_2 = 1 \tag{2}$$

$$f_1 \times R_1 + f_2 \times R_2 = R_S \tag{3}$$

where f_1 and f_2 are the contributions of baseline sediments and dust-contaminated soils, respectively; R_1 and R_2 are the $^{207}Pb/^{206}Pb$ in baseline sediments (0.7971) and dust-contaminated soils (0.8829), respectively; and R_s is the $^{207}Pb/^{206}Pb$ in sediment samples. Pb from dust-contaminated soils contributed $80 \pm 6\%$ (n = 7) from -1.26 km upstream to 2.90 km downstream of the smelter, and 81% in the Seokporicheon tributary (-0.68 km upstream of the smelter, N10). The contribution of dust-contaminated soils decreased to negligible levels in baseline sediments 26.3–44.0 km downstream of the smelter. In contrast, main channel sediments from 44.0 to 90.3 km downstream of the smelter had low Pb concentrations (49.7 ± 15.9 mg/kg, n = 14; Fig. 2d) that were similar to those of baseline sediments, despite high variation in Pb isotope ratios along the Korean ore line, indicating a negligible contribution of Zn smelter-derived materials.

For Zn, sediments near the smelter (-0.55 km upstream to 26.3 km downstream, n = 13) were interpreted as a mixture of dust-contaminated soils (DCS), groundwater-derived Zn (GDZ), and baseline sediments (BS) (Fig. 5b). The Zn isotopic composition of the baseline sediments was divided into two groups, with $\delta^{66}Zn$ of $0.01 \pm 0.07\%$ (n = 10) and $-0.32 \pm 0.06\%$ (n = 5), respectively. The former, main channel sediments from -10.2 to -2.27 km upstream of the smelter (n = 4) and tributary sediments from -10.2 km upstream to 53.0 km downstream of the smelter (n = 7, excluding Seokporichon tributary sediment) were defined as BS1 due to Zn isotopic compositions similar to bulk silicate earth ($-0.04 \pm 0.05\%$, Chen et al 2013). The latter, tributary sediments from 53.0 to 90.3 km downstream of the smelter (n = 5), were defined as BS2 due to lighter Zn isotopic compositions similar to Korean mine ores ($-0.55 \pm 0.08\%$, n = 9) and riverside tailings ($-0.49 \pm 0.04\%$, n = 2). The influence of DCS was apparent near the Zn smelter

($\delta^{66}Zn = -0.18 \pm 0.08\%$, n = 3). GDZ ranges were influenced by isotopic fractionation during Zn leaching from smelting wastes and groundwater Zn adsorption onto Fe-carriers in river sediments. Although Zn released into the environment typically undergoes little isotopic fractionation during dissolution ($\Delta^{66}Zn_{solution-solid} = \sim 0\%$; Desaulty and Petelet-Giraud 2020), isotopic fractionation during adsorption onto iron oxyhydroxide (FeOOH) can reach $\sim 0.29\%$ (Juillot et al. 2008). Based on a recent study of heavy mineral assemblages, the $\delta^{66}Zn$ endmember of GDZ from smelting wastes was estimated to be $1.02 \pm 0.43\%$ (n = 4), as goethite (FeOOH) was abundant in the main channel and tributary sediments examined in this study (MOE 2020b).

Thus, the contribution of each Zn source from -2.27 km upstream to 90.3 km downstream of the smelter was estimated as follows (Zhang et al. 2016):

$$f_1 + f_2 + f_3 = 1 \tag{4}$$

$$f_1 \times R_1 + f_2 \times R_2 + f_3 \times R_3 = R_S \tag{5}$$

$$\frac{f_1 \times C_S}{C_1} + \frac{f_2 \times C_S}{C_2} + \frac{f_3 \times C_S}{C_3} = 1 \tag{6}$$

where f_1, f_2, and f_3 are the contributions of BS1, GDZ, and DCS, respectively, from -2.27 km upstream to 53.0 km downstream of the smelter, and those of BS1, GDZ, and BS2 from 53.0 to 90.3 km, respectively, downstream of the smelter. R_1, R_2, and R_3 are the $\delta^{66}Zn$ values of BS1 (average, 0.01‰, n = 10), GDZ (average, 1.02‰, n = 4), DCS (average, –0.18‰, n = 3), respectively, in the former zone, and BS2 (average, –0.32‰, n = 5) instead of DCS in the latter zone. C_1, C_2, and C_3 are the Zn concentrations in BS1 (average, 476 mg/kg, n = 11), GDZ (estimates 10.000 mg/kg), and DCS (average, 2900 mg/kg, n = 3), respectively, in the former zone, and BS2 (average, 206 mg/kg, n = 5) instead of DCS in the latter zone. C_s and R_s are the measured Zn concentration and $\delta^{66}Zn$ in main channel sediments. Based on the endmember mixing model, BS1 contributed an average of $25 \pm 23\%$ throughout the entire study area, while Zn source materials (DCS + GDZ) from Zn smelter contributed $75 \pm 24\%$ (Fig. 6). Of the two source materials from the Zn smelter, the DCS contributed the most ($64 \pm 16\%$) within a 2 km radius of the smelter (-2.27 km upstream to 1.96 km downstream), with a 33% contribution into the Seokporicheon tributary sediment (N10) at -0.68 km upstream of the smelter. In contrast, the GDZ contributed $55 \pm 15\%$ from -0.55 km upstream to 90.3 km downstream of the smelter and approximately 40% at the entrance of Lake Andong (N58). BS2 from tributaries from 53.0 to 90.3 km downstream of the smelter contributed 11% only at 73.3 km downstream of the smelter (N53). Thus, our heavy metal concentration and isotopic composition analyses estimated
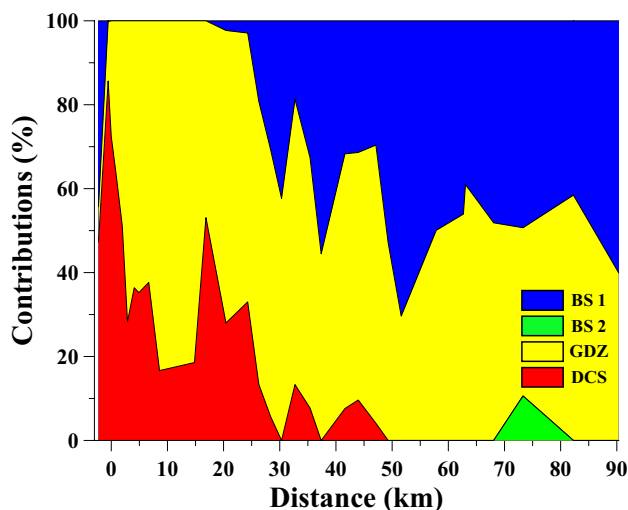
Fig. 6 Contributions (%) of four Zn sources in the main channel sediments. BS 1, BS 2, GDZ, and DCS represent baseline sediment 1 (main channels and tributaries from -10.2 to -0.55 km and -10.2 to 53.0 km, respectively), baseline sediment 2 (tributaries from 53.0 to 90.3 km), groundwater-derived Zn, and dust contaminated soils, respectively

the relative contributions of Pb and Zn contaminant source materials, which allowed us to discriminate the effects of Zn smelting from those of mining tailings, groundwater leaching, and dust-contaminated soils.

Conclusion

This study tried to discriminate the sources and pathways of contaminated Pb and Zn in river sediments influenced by both mining and smelting activities, and to estimate the contribution of each source using stable metal isotopes. Dissolved Zn and Cd concentrations in river waters near the Zn smelter were very high compared to those upstream of the smelter and tributaries, and a cross section near the smelter also showed that the smelter side had much higher concentrations than the road side. This indicates that groundwater with very high Zn and Cd concentrations is discharged into the river. The Pb isotopic compositions of sediments with extremely high Pb concentrations near the smelter were differentiated with those of ores and tailings originating from local mines, and were similar to those of smelter-derived materials such as imported Zn concentrates, residential roof dusts, smelting wastes, and dust-contaminated soils. From the mixing relationships using Pb isotope ratios and Pb concentrations, dust-contaminated soils (DCS) and baseline sediments (BS: tailing contaminated sediments) were regarded as two main contributors of Pb. The $\delta^{66}Zn$ values in the sediments near

the Zn smelter showed an abrupt increase from –0.01 to 0.82‰, which indicate that there are three Zn sources; lighter, heavier and unfractionated Zn such as dust-contamminated soils (DCS, –0.18‰ of $\delta^{66}Zn$), groundwater derived Zn (GDZ, 1.02‰ of $\delta^{66}Zn$) by leaching of smelting wastes stored inside the smelter, and tailings contaminated sediments (BS, 0.01‰ of $\delta^{66}Zn$) from nearby abandoned mines, respectively. The contribution of each source for Pb and Zn in sediments was estimated using two (Pb) and three (Zn) components mixing models. In sediments within 2 km of the Zn smelter, DCS contributed about 78% and 64% for Pb and Zn, respectively, which decreased to negligible levels after 47.1 km downstream. GDZ, another smelter derived Zn, contributed about 54% of total Zn in main channel sediments downstream of the smelter, and contributed over a longer distances than DCS. This is because parts of GDZ were transported in the dissolved phase while DCS was supplied into the river only in the particulate phase. BS for Pb and Zn contributed lowest within 2 km of the smelter and increased from 47.1 km to the entrance of Lake Andong. Environmental forensic studies using metal stable isotopes could be used for the development of environmental management plans in the catchment, and for the assessment for the impacts of mining and smelting activities on the Lake Andong.

Authors contributions Dong-Jin Joe: Investigation, Original draft, Visualization.

Man-Sik Choi: Supervision, Conceptualization, Funding acquisition, Methodology, Writing – review & editing.

Jong-Hyeon Lee: Funding acquisition, Methodology, Validation.

Chan-Kook Kim: Investigation, Methodology, Resources.

Min-Seok Choi: Investigation.

Hyung-Seon Shin: Investigation.

Data availability Not applicable.

Declarations

Ethical approval Not applicable.

Consent to participate Not applicable.

Consent to publish Not applicable.

References

Aranda S, Borrok DM, Wanty RB, Balistrieri LS (2012) Zinc isotope investigation of surface and pore waters in a mountain watershed impacted by acid rock drainage. Sci Total Environ 420:202–213

Araújo DF, Boaventura GR, Machado W, Viers J, Weiss D, Patchineelam SR, Ruiz I, Rodrigues APC, Babinski M, Dantas E (2017) Tracing of anthropogenic zinc sources in coastal environments using stable isotope composition. Chem Geol 449:226–235

Arnold T, Schönbächler M, Rehkämper M, Dong S, Zhao FJ, Kirk GJ, Coles BH, Weiss DJ (2010) Measurement of zinc stable isotope ratios in biogeochemical matrices by double-spike MC-ICPMS and determination of the isotope ratio pool available for plants from soil. Anal Bioanal Chem 398:3115–3125

Bindler R, Renberg I, Klaminder J, Emteryd O (2004) Tree rings as Pb pollution archives? A comparison of 206Pb/207Pb isotope ratios in pine and other environmental media. Sci Total Environ 319(1–3):173–183

Borrok DM, Gieré R, Ren M, Landa ER (2010) Zinc isotopic composition of particulate matter generated during the combustion of coal and coal+ tire-derived fuels. Environ Sci Technol 44(23):9219–9224

Byrne P, Hudson-Edwards KA, Bird G, Macklin MG, Brewer PA, Williams RD, Jamieson HE (2018) Water quality impacts and river system recovery following the 2014 Mount Polley mine tailings dam spill, British Columbia, Canada. Appl Geochem 91:64–74

Chen H, Savage PS, Teng FZ, Helz RT, Moynier F (2013) Zinc isotope fractionation during magmatic differentiation and the isotopic composition of the bulk Earth. Earth Planet Sci Lett 369:34–42

Chen S, Liu Y, Hu J, Zhang Z, Hou Z, Huang F, Yu H (2016) Zinc isotopic compositions of NIST SRM 683 and whole-rock reference materials. Geostand Geoanal Res 40(3):417–432

Chen Z, Ding Y, Jiang X, Duan H, Ruan X, Li Z, Li Y (2022) Combination of UNMIX, PMF model and Pb-Zn-Cu isotopic compositions for quantitative source apportionment of heavy metals in suburban agricultural soils. Ecotoxicol Environ Saf 234:113369

Choi MS, Uoo JS, Kim DS (2007a) Sources identification of anthropogenic Pb in Ulleung basin sediments using stable Pb isotope ratios, East/Japan Sea. Sea J Kor Soc Ocean 12(4): 315–327. In Korean with English abstract

Choi MS, Yi HI, Yang SY, Lee CB, Cha HJ (2007b) Identification of Pb sources in Yellow Sea sediments using stable Pb isotope ratios. Mar Chem 107(2):255–274

Choi M, Park J, Cho D, Jang D, Kim M, Choi J (2015) Tracing metal sources in core sediments of the artificial lake An-Dong, Korea: concentration and metal association. Sci Total Environ 527:384–392

Cumming GL, Richards JR (1975) Ore lead isotope ratios in a continuously changing Earth. Earth Planet Sci Lett 28(2):155–171

Deng J, Wang C, Bagas L, Selvaraja V, Jeon H, Wu B, Yang L (2017) Insights into ore genesis of the Jinding Zn–Pb deposit, Yunnan Province, China: Evidence from Zn and in-situ S isotopes. Ore Geol Rev 90:943–957

Desaulty AM, Petelet-Giraud E (2020) Zinc isotope composition as a tool for tracing sources and fate of metal contaminants in rivers. Sci Total Environ 728:138599

Dickin AP (1995) Isotope geochemistry of oceanic volcanics. Radiogenic Isotope Geology, Cambridge Univ. Press, Edinburgh 1–452

Duan J, Tang J, Lin B (2016) Zinc and lead isotope signatures of the Zhaxikang PbZn deposit, South Tibet: Implications for the source of the ore-forming metals. Ore Geol Rev 78:58–68

Duarte EB, Neves MA, de Oliveira FB, Martins ME, de Oliveira CHR, Burak DL, Orlando MTD, Rangel CVGT (2021) Trace metals in Rio Doce sediments before and after the collapse of the Fundão iron ore tailing dam. Southeastern Brazil Chemosphere 262:127879

Foucher D, Ogrinc, Hintelmann HH (2009) Tracing mercury contamination from the Idrija mining region (Slovenia) to the Gulf of Trieste using Hg isotope ratio measurements. Environ Sci Technol 43(1):33–39

Gagnevin D, Boyce AJ, Barrie CD, Menuge JF, Blakeman RJ (2012) Zn, Fe and S isotope fractionation in a large hydrothermal system. Geochim Cosmochim Acta 88:183–198

Hong YP, Choi JH, Kim YJ, Kim DI, Ryoo KS (2016) Contamination status of the upper Nakdong riverside by heavy metals in mine tailings. Journal of the Korean Society for Environmental Analysis 19(3):135–145. In Korean with English abstract

Horowitz AJ (1991) A primer on sediment-trace element chemistry. Lewis, Boca Raton

Jeon SK, Kwon MJ, Yang JS, Lee S (2017) Identifying the source of Zn in soils around a Zn smelter using Pb isotope ratios and mineralogical analysis. Sci Total Environ 601:66–72

Jeong YJ, Cheong CS, Shin D, Lee KS, Jo HJ, Gautam MK, Lee I (2012) Regional variations in the lead isotopic composition of galena from southern Korea with implications for the discrimination of lead provenance. J Asian Earth Sci 61:116–127

John SG, Park JG, Zhang Z, Boyle EA (2007) The isotopic composition of some common forms of anthropogenic zinc. Chem Geol 245(1–2):61–69

John SG, Rouxel OJ, Craddock PR, Engwall AM, Boyle EA (2008) Zinc stable isotopes in seafloor hydrothermal vent fluids and chimneys. Earth Planet Sci Lett 269(1–2):17–28

Jouvin D, Weiss DJ, Mason TFM, Bravin MN, Louvat P, Zhao F, Ferec F, Hinsinger P, Benedetti MF (2012) Stable isotopes of Cu and Zn in higher plants: evidence for Cu reduction at the root surface and two conceptual models for isotopic fractionation processes. Environ Sci Technol 46(5):2652–2660

Juillot F, Maréchal C, Ponthieu M, Cacaly S, Morin G, Benedetti M, Hazemann JL, Proux O, Guyot F (2008) Zn isotopic fractionation caused by sorption on goethite and 2-Lines ferrihydrite. Geochim Cosmochim Acta 72(19):4886–4900

Kang MJ, Kwon YK, Yu S, Lee PK, Park HS, Song N (2019) Assessment of Zn pollution sources and apportionment in agricultural soils impacted by a Zn smelter in South Korea. J Hazard Mater 364:475–487

Kavner A, John SG, Sass S, Boyle EA (2008) Redox-driven stable isotope fractionation in transition metals: Application to Zn electroplating. Geochim Cosmochim Acta 72(7):1731–1741

Kelley KD, Wilkinson JJ, Chapman JB, Crowther HL, Weiss DJ (2009) Zinc isotopes in sphalerite from base metal deposits in the Red Dog district, northern Alaska. Econ Geol 104(6):767–773

Kim JW, Jung MC, Lee H, Kim H, Heo H (2022) Status and Evaluation of Characteristics of Deposited Tailings in the Upstream of Andong Dam. J Korean Soc Mineral Energy Resour Eng 59(6):607–618. In Korean with English abstract

Kim J, Choi U, Baek SH, Choi HB, Lee J (2016) A study on chemical compositions of sediment and surface water in Nakdong river for tracing contaminants from mining activities. J Korean Earth Sci Soc 37(4):211–217. In Korean with English abstract

Klaminder J, Farmer JG, MacKenzie AB (2011) The origin of lead in the organic horizon of tundra soils: Atmospheric deposition, plant translocation from the mineral soil or soil mineral mixing? Sci Total Environ 409(20):4344–4350

Kwon HW, Kim YH, Kim JJ (2022) Heavy Metal Characteristics of Fish in Watersheds of the Upper Region of the Nakdong River. J Environ Sci Intl 31(2):103–116

Liu J, Zhou Y, She J, Tsang DC, Lippold H, Wang J, Song L (2020) Quantitative isotopic fingerprinting of thallium associated with potentially toxic elements (PTEs) in fluvial sediment cores with multiple anthropogenic sources. Environ Pollut 266:115252

Maréchal CN, Télouk P, Albarède F (1999) Precise analysis of copper and zinc isotopic compositions by plasma-source mass spectrometry. Chem Geol 156(1–4):251–273

Mason TF, Weiss DJ, Chapman JB, Wilkinson JJ, Tessalina SG, Spiro B, Spiro B, Horstwood MSA, Spratt J, Coles BJ (2005) Zn and Cu isotopic variability in the Alexandrinka volcanic-hosted massive sulphide (VHMS) ore deposit, Urals Russia. Chem Geol 221(3–4):170–187

Mason TF, Weiss DJ, Horstwood M, Parrish RR, Russell SS, Mullane E, Coles BJ (2004) High-precision Cu and Zn isotope analysis by plasma source mass spectrometry Part 1. Spectral interferences and their correction. J Anal Atom Spectrom 19(2):209–217

Mattielli N, Petit JC, Deboudt K, Flament P, Perdrix E, Taillez A, Rimetz-Planchon J, Weis D (2009) Zn isotope study of atmospheric emissions and dry depositions within a 5 km radius of a Pb–Zn refinery. Atmos Environ 43(6):1265–1272

Ministry of Environment (MOE) (2016) Environmental impact survey in the vicinity of Seokpo smelter. M082186:1–414

Ministry of Environment (MOE) (2020a) Seokpo smelter ground water heavy metal contamination causes and leakage investigation. M090007:1–216

Ministry of Environment (MOE) (2020b) Research on water and sediment quality at the upstream region of Andong Dam (II). 1–603

Mondillo N, Wilkinson JJ, Boni M, Weiss DJ, Mathur R (2018) A global assessment of Zn isotope fractionation in secondary Zn minerals from sulfide and non-sulfide ore deposits and model for fractionation control. Chem Geol 500:182–193

Monna F, Lancelot J, Croudace IW, Cundy AB, Lewis JT (1997) Pb isotopic composition of airborne particulate material from France and the southern United Kingdom: implications for Pb pollution sources in urban areas. Environ Sci Technol 31(8):2277–2286

Morton-Bermea O, Rodríguez-Salazar MT, Hernández-Alvarez E, García-Arreola ME, Lozano-Santacruz R (2011) Lead isotopes as tracers of anthropogenic pollution in urban topsoils of Mexico City. Geochemistry 71(2):189–195

Mukai H, Furuta N, Fujii T, Ambe Y, Sakamoto K, Hashimoto Y (1993) Characterization of sources of lead in the urban air of Asia using ratios of stable lead isotopes. Environ Sci Technol 27(7):1347–1356

National Institute of Environmental Research (NIER) (2011) A study on tracking sources of pollutants using environmental forensics techniques (I). N028844:1–32

Nieuwenhuize J, Maas YE, Middelburg JJ (1994) Rapid analysis of organic carbon and nitrogen in particulate materials. Mar Chem 45(3):217–224

Ochoa Gonzalez R, Weiss D (2015) Zinc isotope variability in three coal-fired power plants: a predictive model for determining isotopic fractionation during combustion. Environ Sci Technol 49(20):12560–12567

Park JJ, Kim KJ, Yoo SM, Kim EH, Seok KS, Shin HS, Kim YH (2012) Tracking lead contamination sources of sediments in Lake Andong using lead isotopes. Anal Sci Technol 25(6):429–434. In Korean with English abstract

Park KH, Chang HW (2005) Pb isotopic composition of Yeonhwa and Janggun Pb-Zn ore deposits and origin of Pb: role of Precambrian crustal basement and Mesozoic igneous rocks. J Petrol Soc Korea 14(3):141–148. In Korean with English abstract

Pašava J, Tornos F, Chrastný V (2014) Zinc and sulfur isotope variation in sphalerite from carbonate-hosted zinc deposits, Cantabria, Spain. Miner Deposita 49:797–807

Shiel AE, Weis D, Orians KJ (2010) Evaluation of zinc, cadmium and lead isotope fractionation during smelting and refining. Sci Total Environ 408(11):2357–2368

Šillerová H, Chrastný V, Vítková M, Francová A, Jehlička J, Gutsch MR, Kocourková J, Aspholm PE, Nilsson LO, Berglen TF, Jensen HKB, Komárek M (2017) Stable isotope tracing of Ni and Cu pollution in North-East Norway: Potentials and drawbacks. Environ Pollut 228:149–157

Sivry Y, Riotte J, Sonke JE, Audry S, Schäfer J, Viers J, Blanc G, Freydier R, Dupré B (2008) Zn isotopes as tracers of anthropogenic pollution from Zn-ore smelters The Riou Mort-Lot River system. Chem Geol 255(3–4):295–304

Skierszkan EK, Mayer KU, Weis D, Beckie RD (2016) Molybdenum and zinc stable isotope variation in mining waste rock drainage and waste rock at the Antamina mine, Peru. Sci Total Environ 550:103–113

Song IG, Kang YG, Kim JH, Yoon H, Um WY, Chang YS (2023) Assessment of sulfidated nanoscale zerovalent iron for in-situ remediation of cadmium-contaminated acidic groundwater at a zinc smelter. J Hazard Mater 441:129915

Sonke JE, Sivry Y, Viers J, Freydier R, Dejonghe L, André L, Aggarwal JK, Fontan F, Dupré B (2008) Historical variations in the isotopic composition of atmospheric zinc deposition from a zinc smelter. Chem Geol 252(3–4):145–157

Souto-Oliveira CE, Babinski M, Araújo DF, Andrade MDF (2018) Multi-isotopic fingerprints (Pb, Zn, Cu) applied for urban aerosol source apportionment and discrimination. Sci Total Environ 626:1350–1366

Tanimizu M, Asada Y, Hirata T (2002) Absolute isotopic composition and atomic weight of commercial zinc using inductively coupled plasma mass spectrometry. Anal Chem 74(22):5814–5819

Todt W, Cliff RA, Hanser A, Hofmann AW (1996) Evaluation of a 202Pb–205Pb double spike for high-precision lead isotope analysis. In: Basu AR, Hart SR (eds) Earth Processes: Reading the Isotopic Code. Am Geophys Union, USA, pp 429–437

Tonhá MS, Garnier J, Araújo DF, Cunha BC, Machado W, Dantas E, Araújo R, Kutter VT, Bonnet MP, Seyler P (2020) Behavior of metallurgical zinc contamination in coastal environments: A survey of Zn from electroplating wastes and partitioning in sediments. Sci Total Environ 743:140610

Townsend AT, Seen AJ (2012) Historical lead isotope record of a sediment core from the Derwent River (Tasmania, Australia): A multiple source environment. Sci Total Environ 424:153–161

Verardo DJ, Froelich PN, McIntyre A (1990) Determination of organic carbon and nitrogen in marine sediments using the Carlo Erba NA-1500 Analyzer. Deep Sea Research Part A. Oceanographic Research Papers 37(1):157–165

Vrhovnik P, Smuc NR, Dolenec T, Serafimovski T, Dolenec M (2013) Impact of Pb-Zn mining activity on surficial sediments of Lake Kalimanci (FYR Macedonia). Turkish J Earth Sci 22(6):996–1009

Wang L, Jin Y, Weiss DJ, Schleicher NJ, Wilcke W, Wu L, Guo Q, Chen J, O'Connor D, Hou D (2021) Possible application of stable isotope compositions for the identification of metal sources in soil. J Hazard Mater 407:124812

Weiss DJ, Rausch N, Mason TF, Coles BJ, Wilkinson JJ, Ukonmaanaho L, Arnold T, Nieminen TM (2007) Atmospheric deposition and isotope biogeochemistry of zinc in ombrotrophic peat. Geochim Cosmochim Acta 71(14):3498–3517

Weiss D, Shotyk W, Kramers JD, Gloor M (1999) Sphagnum mosses as archives of recent and past atmospheric lead deposition in Switzerland. Atmos Environ 33(23):3751–3763

Wilkinson JJ, Weiss DJ, Mason TFD, Coles BJ (2005) Zinc isotope variation in hydrothermal systems: preliminary evidence from the Irish Midlands ore field. Econ Geol 100(3):583–590

Yin NH, Sivry Y, Benedetti MF, Lens PN, van Hullebusch ED (2016) Application of Zn isotopes in environmental impact assessment

of Zn–Pb metallurgical industries: a mini review. Appl Geochem 64:128–135

Zhang R, Guan M, Shu Y, Shen L, Chen X, Zhang F, Li T, Jiang T (2016) Reconstruction of historical lead contamination and sources in Lake Hailing, Eastern China: a Pb isotope study. Environ Sci Pollut Res 23:9183–9191

Zhang Y, Runsheng H, Lei W, Wei P (2022) Zn–S isotopic fractionation effect during the evolution process of ore-forming fluids: A case study of the ultra-large Huize rich Ge-bearing Pb–Zn deposit. Appl Geochem 140:105240

Zhao X, He B, Wu H, Zheng G, Ma X, Liang J, Li P, Fan Q (2020) A comprehensive investigation of hazardous elements contamination in mining and smelting-impacted soils and sediments. Ecotoxicol Environ Saf 192:110320

Zhong Q, Yin M, Zhang Q, Beiyuan J, Liu J, Yang X, Wang J, Wang L, Jiang Y, Xiao T, Zhang Z (2021) Cadmium isotopic fractionation in lead-zinc smelting process and signatures in fluvial sediments. J Hazard Mater 411:125015

Zhu C, Liao S, Wang W, Zhang Y, Yang T, Fan H, Wen H (2018) Variations in Zn and S isotope chemistry of sedimentary sphalerite, Wusihe Zn-Pb deposit, Sichuan Province, China. Ore Geol Rev 95:639–648

Žibret G, Šajn R (2008) Modelling of atmospheric dispersion of heavy metals in the Celje area Slovenia. J Geochem Explor 97(1):29–41